

**Biophysical Journal, Volume 113**

**Supplemental Information**

**Catch Bonds at T Cell Interfaces: Impact of Surface Reorganization and  
Membrane Fluctuations**

**Robert H. Pullen, III and Steven M. Abel**

# Supporting Material

## Catch bonds at T cell interfaces: Impact of surface reorganization and membrane fluctuations

Robert H. Pullen III and Steven M. Abel

Department of Chemical and Biomolecular Engineering,  
National Institute for Mathematical and Biological Synthesis  
University of Tennessee, Knoxville, Tennessee 37996, USA

### 1 Parameterization of TCR lifetime data

Parameters for Eqns. 1 and 2 in the paper were obtained by a nonlinear least squares fit of the lifetime data from Liu et al. (1):

	$k_0$ ( $s^{-1}$ )	$f_0$ (pN)	$k_c$ ( $s^{-1}$ )	$f_c$ (pN)	$k_s$ ( $s^{-1}$ )	$f_s$ (pN)
OVA	—	—	4.241	3.150	0.374	9.280
A2	—	—	3.610	4.466	0.735	10.460
E1	2.514	5.533	—	—	—	—

## 2 Methods: Determination of time step and system size

The explicit finite difference method is conditionally stable and relies on the relation between the dimensionality, spatial discretization, and time step of the system. The Courant-Friedrichs-Lewy (CFL) condition imposes a recurrence relation that relates the spatial discretization of a lattice to the time step for the general  $N$ -dimensional heat equation. However, with the addition of the advection term, it is necessary to consider additional stability arguments (2). For a general advection-diffusion PDE of the form

$$\frac{\partial \phi(\vec{x}, t)}{\partial t} = \sum_{i=1}^N \left( D_i \frac{\partial^2 \phi}{\partial x_i^2} - u_i \frac{\partial \phi}{\partial x_i} \right),$$

both of the following conditions must be met to maintain numerical stability with a forward-time central-space scheme

$$(i) \sum_{i=1}^N \frac{2D_i \Delta t}{(\Delta x_i)^2} \leq 1 \quad \text{and} \quad (ii) \sum_{i=1}^N \frac{u_i^2 \Delta t}{2D_i} \leq 1.$$

The first inequality implies the CFL condition and is more restrictive for a diffusion-dominated system. The second inequality is more restrictive for an advection-dominated system. While these conditions do not map directly to our system as  $E_p$  depends on the changing intermembrane distance profile, they provide a good baseline to test for a stable time step that can be verified through subsequent simulations. After assuming an extreme case in which numerical instability is most likely (the initial time point in our simulations), we calculate the appropriate time step as a function of the compressional stiffness at a given lattice spacing (Fig. S1).

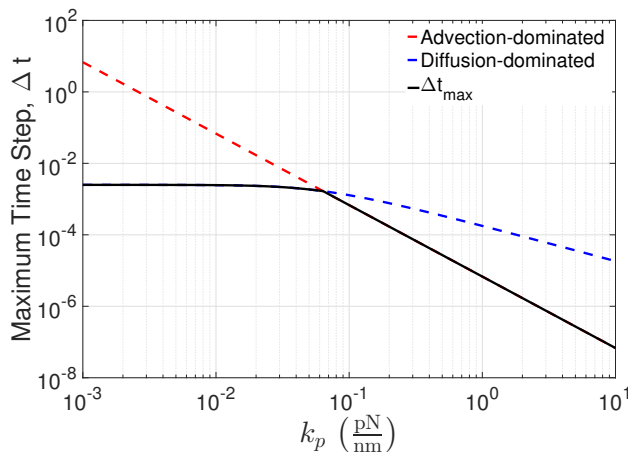


Fig. S1: Maximum time step as a function of the compressional stiffness ( $k_p$ ) given a lattice spacing of 10 nm.

In addition to evaluating the time step, it is important to ensure that finite-size effects do not have an impact on the simulation results. We ran ten individual trajectories at several system sizes and calculated the effective depletion zone diameters at  $t = 1$  s. There was no significant difference in the depletion zone diameter for periodic domains larger than  $400 \text{ nm} \times 400 \text{ nm}$ .

### 3 Dynamics with $\beta \rightarrow \infty$ (no thermal fluctuations)

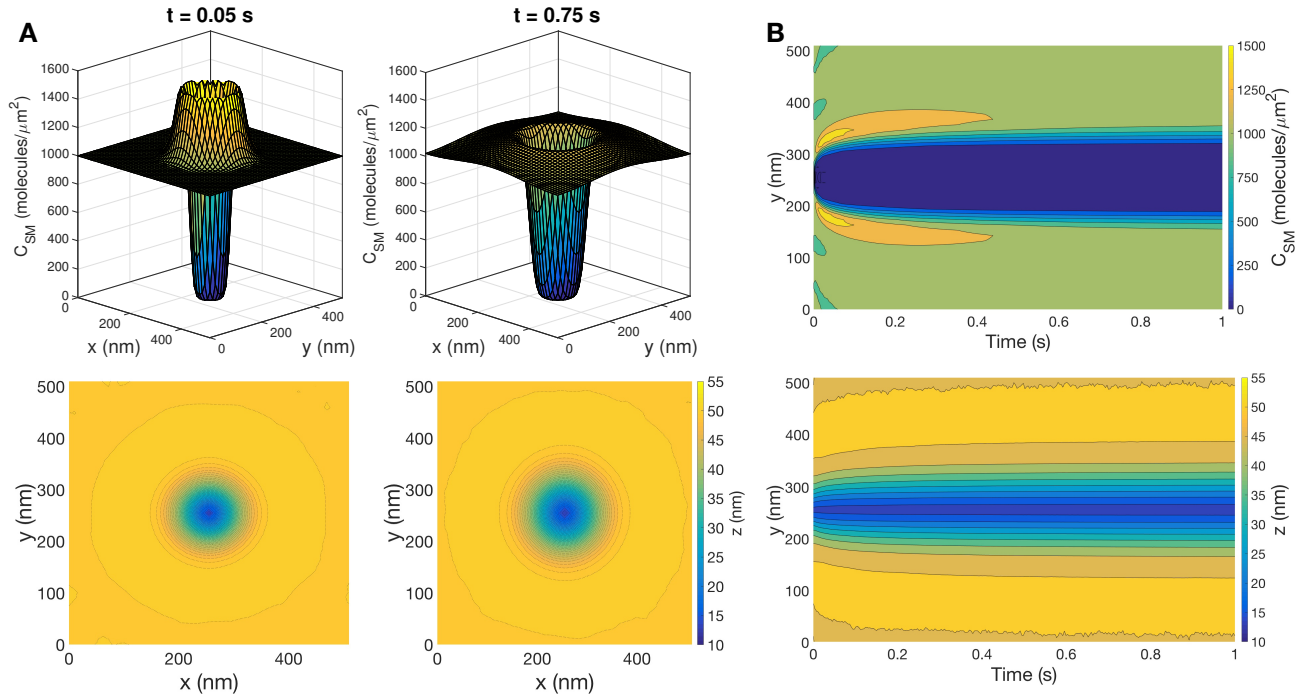


Fig. S2: Characteristic response to the formation of a bond without thermal fluctuations. (A) Snapshots of  $C_{SM}$  (top row) and  $z$  (bottom row) with  $\kappa = 12.15 k_B T$ . Each column corresponds to a different time point. The bond is located at the center of the domain. (B) Kymographs of  $C_{SM}$  and  $z$  from a one-dimensional slice containing the bond.



## 4 Effective off rates

Here, we present results obtained by numerically evaluating Eqn. 7 from the paper. Given an average force ( $f_A$ ) on a bond, we compute the ratio of the effective off rate (averaged over fluctuations) to the off rate  $k_{\text{off}}(f_A)$ . We compute the quantity for OVA, A2, and E1 assuming that  $k_{\text{off}}(-f) = k_{\text{off}}(f)$  and using the standard deviations obtained from simulations.

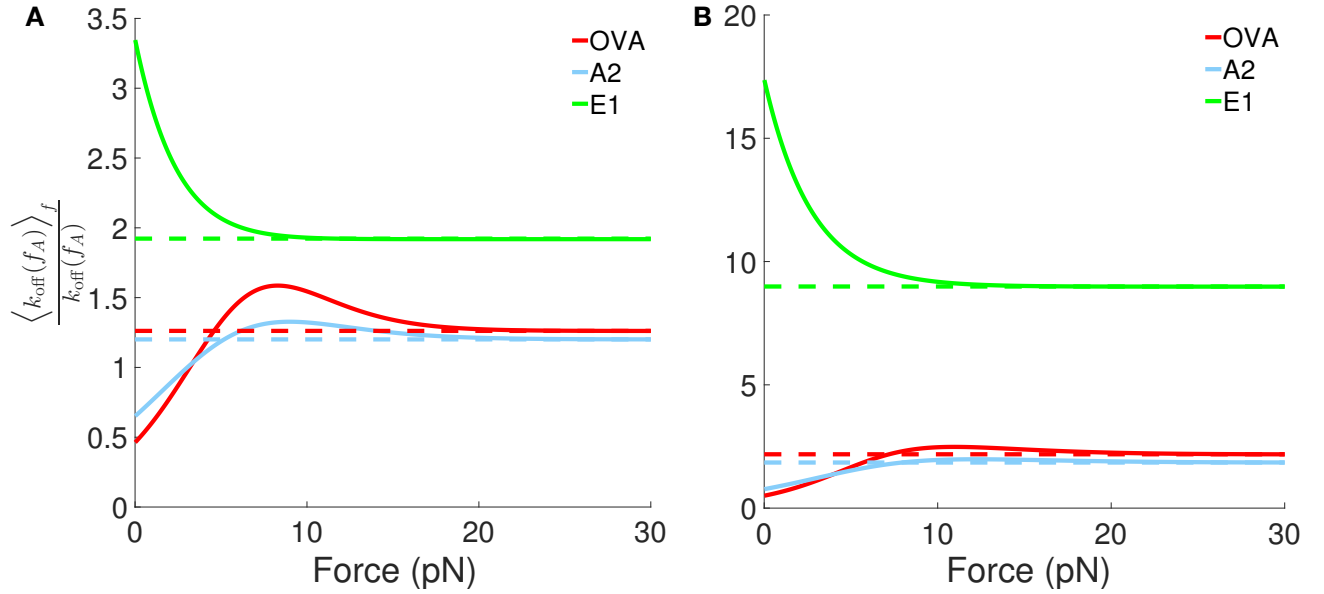


Fig. S3: Ratio of the effective off rate to  $k_{\text{off}}(f_A)$  for different ligands. Solid lines are obtained by numerically integrating Eqn. 7 from the paper. Dashed lines are analytical results obtained in the limit  $f \gg f_c$ . (A)  $\kappa = 12.15 k_B T$ . (B)  $\kappa = 40 k_B T$ .

## 5 Variation of catch bond parameters

Survival probabilities in the main text were obtained using parameters from fits of lifetime data for three different ligands. Here, we take the four parameters associated with the catch bond OVA and independently vary two of the parameters while holding the other two fixed. This provides a broader view of how the parameters affect the survival of a bond.

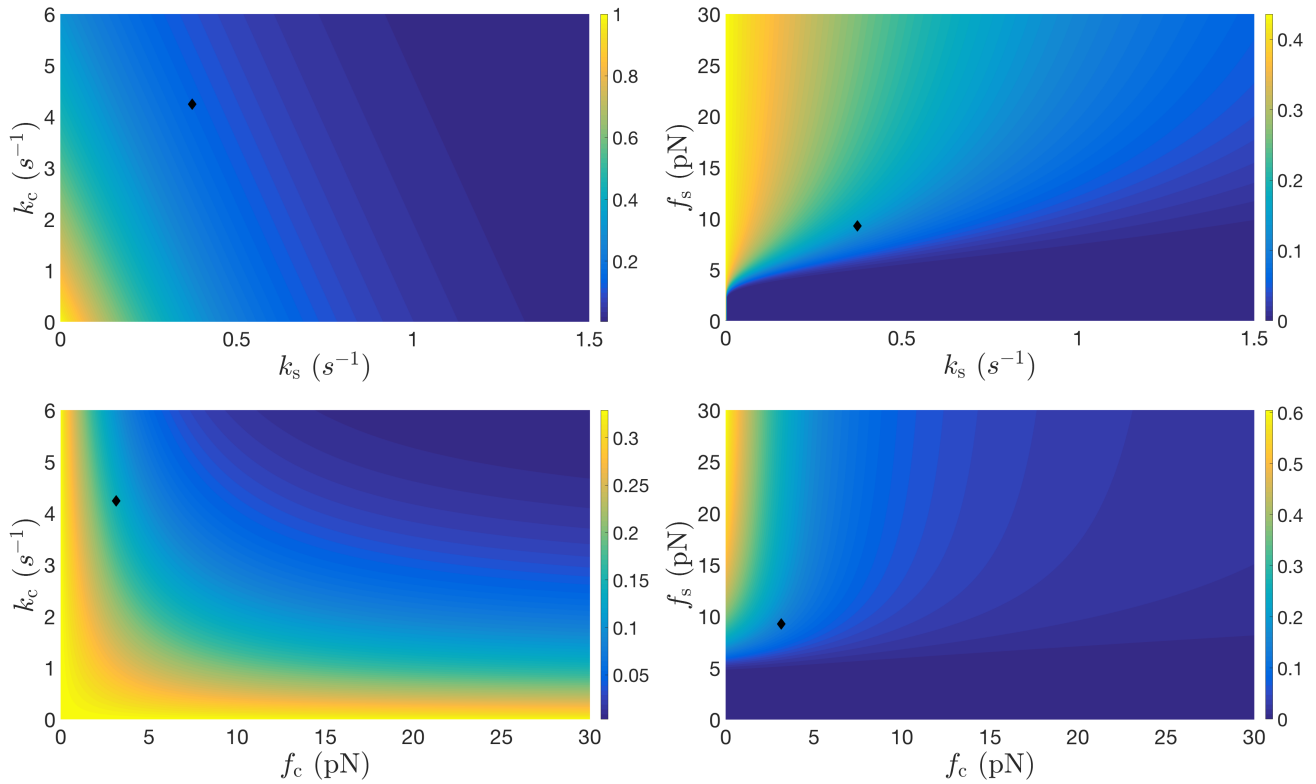


Fig. S4: The fraction of bonds that remain at  $t = 1$  s ( $\phi$ ) as two parameters are varied in the catch-bond model (Eqn. 2). Other parameters are fixed at values associated with OVA. Black diamonds correspond to parameters used in the main text for OVA. The survival fraction at each combination of parameters is calculated by averaging ten independent survival curves with  $\kappa = 12.15 k_B T$ .

## 6 Survival probabilities with alternative definitions of $k_{\text{off}}$

To our knowledge, there has been no extensive discussion regarding the lifetimes of catch bonds or slip bonds under compressive forces. Here, we compare the resulting survival probabilities for three different assumptions about the behavior of Eqns. 1 and 2 under compressive forces. For  $f \geq 0$ , the off rates are equivalent to those defined in the main text:  $k_{\text{off}}^{\text{case } i}(f) = k_{\text{off}}(f)$ , where  $i$  denotes the specific case and  $k_{\text{off}}$  on the right-hand side corresponds to either Eqn. 1 (slip) or 2 (catch) in the main text. For compressive forces ( $f < 0$ ), the three cases are

$$\left. \begin{aligned} k_{\text{off}}^{\text{case } 1}(f) &= k_{\text{off}}(-f) \\ k_{\text{off}}^{\text{case } 2}(f) &= k_{\text{off}}(0) \\ k_{\text{off}}^{\text{case } 3}(f) &= k_{\text{off}}(f) \end{aligned} \right\} \text{ for } f < 0$$

In the main text, we assume off rates satisfy case 1 and are even functions of the force. Figure S5 shows differences between the three cases that emerge when evaluating survival probabilities for a single bond (A), for two bonds separated by 40 nm (B), and for a single bond without surface molecules (C). The prevalence of negative forces increases from A to C.

The slip bond E1 shows a substantial change between the different off-rate cases only when surface molecules are absent ( $\langle f \rangle = 0$ ) and negative forces are common (Fig. S5, panel C). Comparing case 2 to case 1, the survival probabilities for catch bonds decrease slightly in A and B and decrease more significantly if long surface molecules are excluded (C). For case 3, there are large deviations for catch bonds in A, B, and C. This is because the catch bond equations for OVA and A2 lead to a rapid decrease in average lifetime with increasing compressive force. This case is likely unphysical.

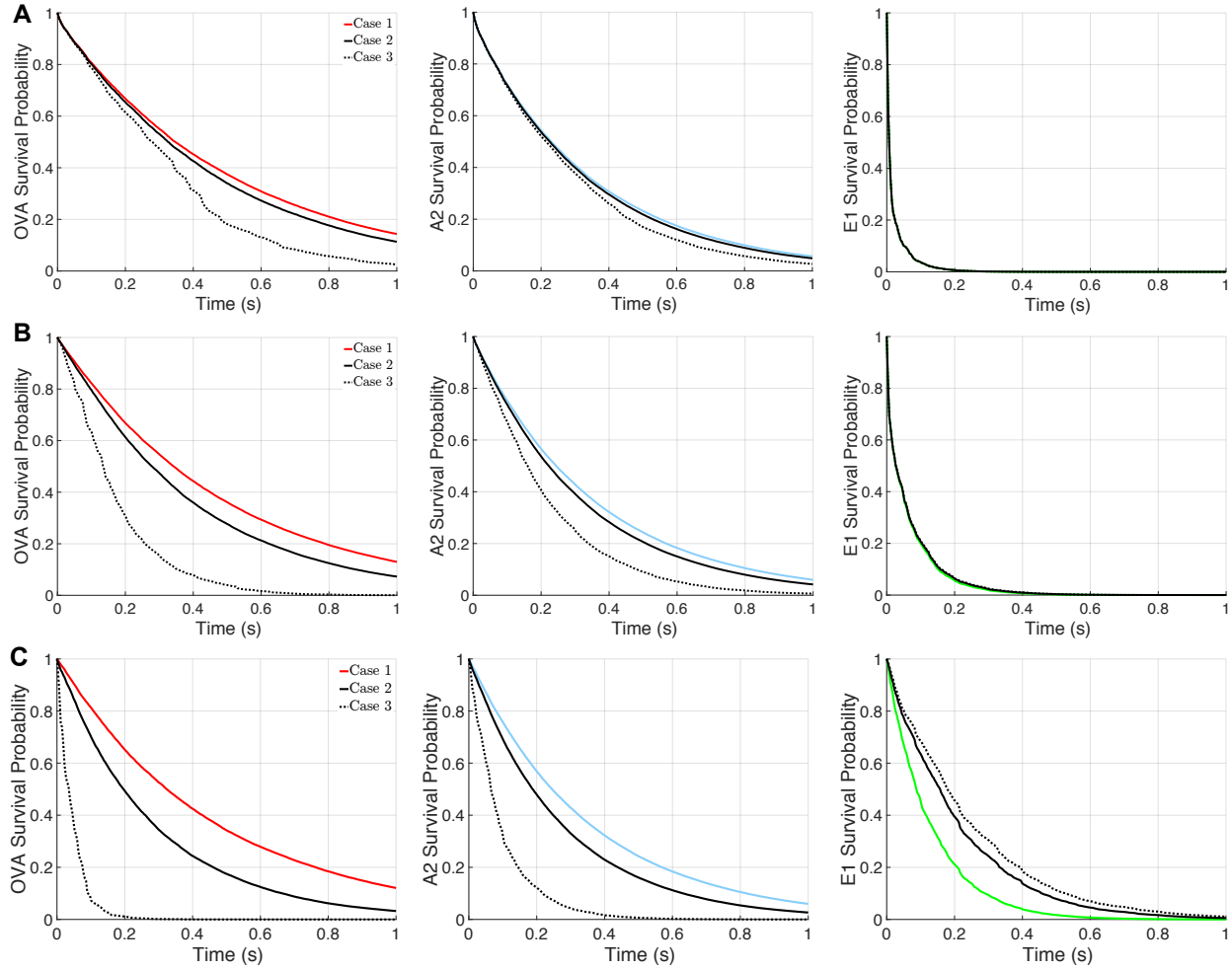


Fig. S5: Survival probabilities with different treatments of compressive forces ( $\kappa = 12.15 k_B T$  with thermal fluctuations). Each column corresponds to a different ligand and each row to a different physical system: (A) a single bond; (B) two bonds separated by 40 nm; (C) a single bond in a system with no other surface molecules ( $C_{SM} = 0$ ). Compressive forces are treated according to the three cases described above. Case 1 corresponds to results from the main text. Each survival probability curve is calculated by averaging ten independent survival curves.

## 7 Variation of $z_0$ and $z_p$

In this section, we examine effects of either increasing the TCR-pMHC bond length ( $z_0$ ) or decreasing the length of long surface molecules ( $z_p$ ). Both increasing  $z_0$  and decreasing  $z_p$  lead to smaller average bond tensions (Fig. S6) and longer bond lifetimes (Fig. S7), although the catch bond lifetimes are minimally affected at  $\kappa = 12.15 k_B T$ . Because of the form of Eqn. 3 in the main text, the difference in lengths,  $z_p - z_0$ , governs the bond tension. A decrease in surface molecule length is equivalent to an equal increase in TCR-pMHC bond length, which is consistent with analysis from Allard et al. (3).

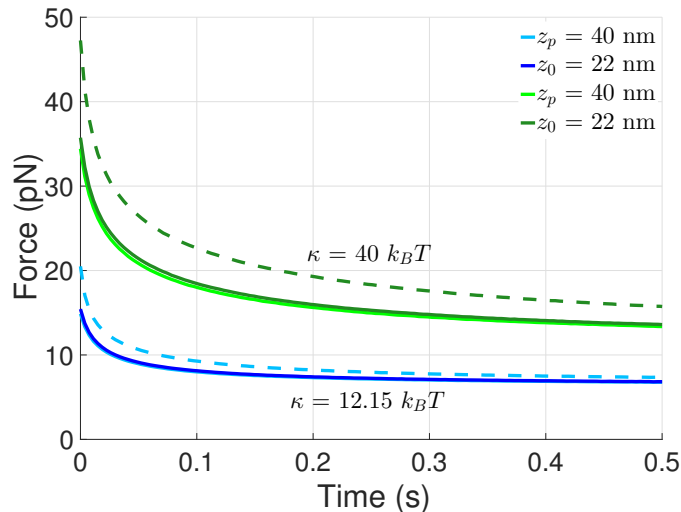


Fig. S6: Average bond tension as a function of time for a single bond without thermal fluctuations. The average tension at each time point is calculated by averaging the tension from ten independent simulation trajectories. Dashed lines correspond to conditions presented in the main text ( $z_0 = 13$  nm,  $z_p = 50$  nm). Darker shades are associated with a longer TCR-pMHC bond ( $z_0 = 22$  nm,  $z_p = 50$  nm). Lighter shades are associated with a decreased length of long surface molecules ( $z_0 = 13$  nm,  $z_p = 40$  nm). Results with thermal fluctuations are not shown.

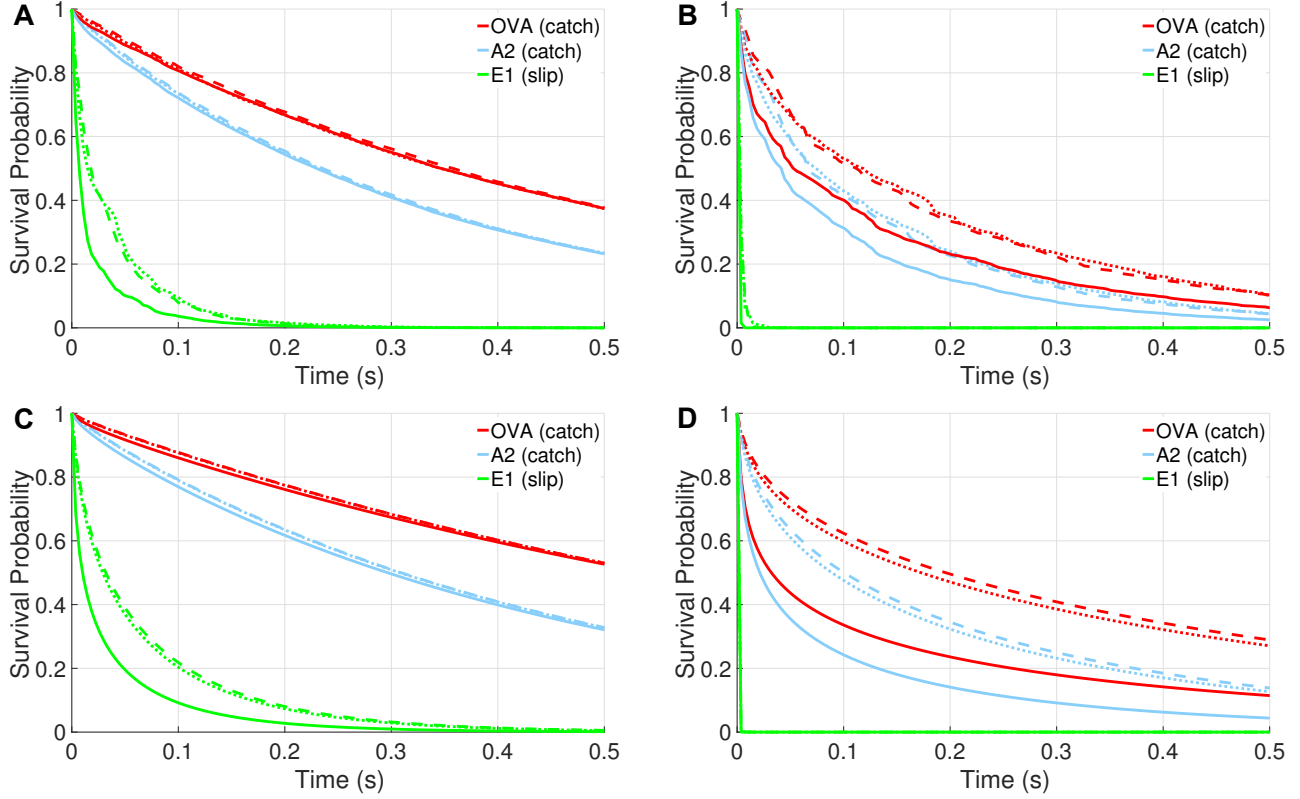


Fig. S7: Survival probabilities for different ligands at conditions presented in the main text (solid lines), with  $z_0 = 22$  nm (dotted lines), and with  $z_p = 40$  nm (dashed lines). Each survival probability curve is calculated by averaging ten independent survival curves. Conditions studied are: (A)  $\kappa = 12.15 k_B T$  with thermal fluctuations; (B)  $\kappa = 40 k_B T$  with thermal fluctuations; (C)  $\kappa = 12.15 k_B T$  without thermal fluctuations; (D)  $\kappa = 40 k_B T$  without thermal fluctuations.

## References

- [1] Liu, B., W. Chen, B. Evavold, and C. Zhu, 2014. Accumulation of Dynamic Catch Bonds between TCR and Agonist Peptide-MHC Triggers T Cell Signaling. *Cell* 157:357–368. [//www.sciencedirect.com/science/article/pii/S0092867414003419](http://www.sciencedirect.com/science/article/pii/S0092867414003419).
- [2] Hindmarsh, A., P. Gresho, and D. Griffiths, 1984. The stability of explicit Euler time-integration for certain finite difference approximations of the multi-dimensional advection–diffusion equation. *Int. J. Numer. Meth. Fluids* 4:853–897.
- [3] Allard, J. F., O. Dushek, D. Coombs, and P. A. van der Merwe, 2012. Mechanical modulation of receptor–ligand interactions at cell–cell interfaces. *Biophys. J.* 102:1265–1273.